

# *Thermotoga maritima* TM0298 is a highly thermostable mannitol dehydrogenase

Seung Hoon Song · Nitasha Ahluwalia · Yvonne Leduc ·  
Louis T. J. Delbaere · Claire Vieille

Received: 16 May 2008 / Revised: 21 July 2008 / Accepted: 28 July 2008 / Published online: 22 August 2008  
© Springer-Verlag 2008

**Abstract** *Thermotoga maritima* TM0298 is annotated as an alcohol dehydrogenase, yet it shows high identity and similarity to mesophilic mannitol dehydrogenases. To investigate this enzyme further, its gene was cloned and expressed in *Escherichia coli*. The purified recombinant enzyme was most active on fructose and mannitol, making it the first known hyperthermophilic mannitol dehydrogenase. *T. maritima* mannitol dehydrogenase (TmMtDH) is optimally active between 90 and 100 °C and retains 63% of its activity at 120 °C but shows no detectable activity at room temperature. Its kinetic inactivation follows a first-order mechanism, with half-lives of 57 min at 80 °C and 6 min at 95 °C. Although TmMtDH has a higher  $V_{\max}$  with NADPH than with NADH, its catalytic efficiency is 2.2 times higher with NADH than with NADPH and 33 times higher with  $\text{NAD}^+$  than with  $\text{NADP}^+$ . This cofactor specificity can be explained by the high density of negatively charged residues (Glu193, Asp195, and Glu196) downstream of the NAD(P) interaction site, the glycine motif. We demonstrate that TmMtDH contains a single catalytic zinc per subunit. Finally, we provide the first proof of concept that mannitol can be produced directly from glucose in a two-step enzymatic process,

using a *Thermotoga neapolitana* xylose isomerase mutant and TmMtDH at 60 °C.

**Keywords** *Thermotoga maritima* · Mannitol dehydrogenase · Thermostable enzyme · Mannitol · Glucose · Fructose

## Introduction

Industrial polyols are sugar alcohols that are widely used in the pharmaceutical, chemical, and food ingredient industries. For example, mannitol is used as a low-caloric and low-cariogenic sweetener (Le and Mulderrig 2001), as a pharmaceutical formulating agent (Le and Mulderrig 2001), and as a specialty chemical in other industrial applications (Soetaert et al. 1995). Currently, 50,000 tons/year of mannitol are produced by the hydrogenation of a 50% fructose/50% glucose syrup at high pressures and temperatures using a Raney nickel catalyst (Kulbe et al. 1987; Soetaert et al. 1999). The fructose/glucose syrup is converted to a 30% mannitol/70% sorbitol mixture from which mannitol is purified by low-temperature crystallization (Soetaert et al. 1999). Because of the low yield and high-energy costs associated with this production process, several biological mannitol production processes are being investigated. A cheaper production process would open the door to new applications for mannitol, and it would create new markets for starch.

In biological systems, mannitol is produced enzymatically from fructose by mannitol dehydrogenase (MtDH, EC 1.1.1.67) using NAD(P)H as the cofactor (Jörnvall et al. 1984, 1987; Schneider and Giffhorn 1989; Slatner et al. 1999). At present, the most promising laboratory fermentation processes for mannitol production use *Leuconostoc*

S. H. Song · N. Ahluwalia · C. Vieille (✉)  
Department of Biochemistry and Molecular Biology,  
Michigan State University,  
110 Biochemistry Building,  
East Lansing, MI 48824, USA  
e-mail: vieille@msu.edu

Y. Leduc · L. T. J. Delbaere  
Department of Biochemistry, University of Saskatchewan,  
Saskatoon, Saskatchewan S7N 5E5, Canada

*mesenteroides*, which can produce up to 150 g/l mannitol (Soetaert et al. 1999) with the following fermentation balance:



High volumetric productivity (26.2 g mannitol/l h<sup>-1</sup>) and yield (0.97 mol/mol fructose consumed) were obtained with *Leuconostoc pseudomesenteroides* resting cells in a membrane cell-recycle bioreactor (von Weymarn et al. 2002). But since one third of the hexose consumed (provided as glucose) is used for cofactor regeneration, the mannitol yield can never be higher than 0.66 mol/mol hexose consumed.

Recently, a whole-cell biotransformation process for direct glucose conversion to mannitol was developed in *Escherichia coli*. It combines an extracellular xylose (glucose) isomerase with a recombinant *E. coli* strain that expresses MtDH and formate dehydrogenase to yield 0.8 mol D-mannitol from 1 mol D-glucose (Kaup et al. 2005). In this process, glucose is first isomerized to fructose by the extracellular xylose isomerase, then reduced to mannitol by MtDH. Added as a co-substrate, formate is oxidized by formate dehydrogenase to regenerate the pyrimidine nucleotide, NADH. The disadvantages of this process are that it uses formate (an expensive chemical) and requires precise pH control.

It is theoretically possible to convert 100% fructose into 100% mannitol using an immobilized enzyme system, as is done today for fructose syrup (42% fructose/58% glucose) production in an immobilized xylose (glucose) isomerase reactor. Because a large selection of thermostable xylose isomerases is available, it is also easy to foresee mannitol production directly from glucose in an immobilized bioreactor system containing xylose isomerase and MtDH. Such a system can be developed if a robust thermostable MtDH is available and if the reduced pyrimidine nucleotide cofactor can easily be regenerated. Electrochemical recycling of pyridine nucleotide cofactors is a promising technology that has already been extensively studied. Many of the potential obstacles (e.g., electrode fouling, cofactor dimerization, and the necessity of high overpotentials) have been overcome through method development (Albery et al. 1987; Bardea et al. 1997; Chen et al. 2001; Gründig et al. 1995; Jaegfeldt et al. 1981; Karyakin et al. 1995; Laurinavicius et al. 1996; Munteanu et al. 2001; Ohtani et al. 1997; Pariente et al. 1995; Park and Zeikus 2003; Park et al. 1999, 2003; Prodomidis and Karayannis 2002; van der Donk and Zhao 2003; Willner and Katz 2000).

Numerous MtDHs have already been characterized for their industrial potential (Aarnikunnas et al. 2002; Brünker et al. 1997; Sasaki et al. 2005; Schafer et al. 1997; Schneider et al. 1993; Stoop and Mooibroek 1998). All of

them are from mesophilic organisms, though, and none is highly thermostable. For this reason, we used a data mining approach to search for MtDH sequences in the genomes of thermophilic and hyperthermophilic organisms. This paper describes the cloning of the *Thermotoga maritima* MtDH-encoding gene, the biochemical characterization of the recombinant enzyme, and the first proof of concept that this enzyme can be used in an efficient biochemical process to convert glucose to mannitol.

## Materials and methods

### Database mining

The amino acid sequence of medium-chain *Leuconostoc mesenteroides* MtDH (GenBank no. AAM09029) was used as the query sequence in a BLASTp search of the proteins encoded by all completed bacterial genomes (at <http://tigrblast.tigr.org/cmr-blast/>). The *T. maritima* TM0298 amino acid sequence was subsequently used as the query sequence in a BLASTp search of GenBank (at <http://www.ncbi.nlm.nih.gov/>). The search results were scored by probability to identify sequences with the highest identity and similarity to the query sequence.

### Strains and media

*T. maritima*, type strain MSB8 (ATCC 43589), was grown in BSMII medium under a N<sub>2</sub> atmosphere (Johnson et al. 2006). Tubes were sealed with septum stoppers and aluminum seals before autoclaving. Trace mineral and vitamin supplements (ATCC, Manassas, VA, USA) were added after autoclaving, and the medium was reduced with a few drops of 2.5% sodium sulfide. Cultures were started with a 1% (v/v) inoculum and were grown overnight at 80 °C in an oil bath (200® Fluid 500 CST, Dow Corning, Midland, MI, USA). *E. coli* strains used in this study were DH5α (Invitrogen, Carlsbad, CA, USA) for cloning and plasmid propagation, and BL21(DE3) (Novagen, Madison, WI, USA) for protein expression. *E. coli* strains were routinely grown in Luria–Bertani medium (Ausubel et al. 1993) in the presence of 50 µg/ml kanamycin when needed for plasmid maintenance. BL21(DE3) was grown in Super Broth (SB; per liter, 12 g bacto-tryptone, 24 g yeast extract, 13 ml glycerol, 15.3 g K<sub>2</sub>HPO<sub>4</sub>, 1.7 g KH<sub>2</sub>PO<sub>4</sub>, and 1 mM MgSO<sub>4</sub>) for protein expression.

### Extraction of *T. maritima* genomic DNA

A 200-ml *T. maritima* culture was harvested by centrifugation for 15 min at 4,000×g, and the cell pellet was washed twice with 50 ml of 50 mM Tris–HCl, 50 mM ethyl-

enediaminetetraacetic acid (EDTA; pH 8.0). The pellet was then resuspended in 15 ml of lysis buffer [50 mM Tris-HCl (pH 8.0), 50 mM EDTA, 0.5% Tween 20, and 0.5% Triton X-100]. RNase (200  $\mu$ l at 10 mg/ml), lysozyme (500  $\mu$ l at 10 mg/ml), and protease K (200  $\mu$ l at 20 mg/ml) were added, and the cell suspension was incubated at 37 °C for 30 min. After adding 4 ml of a 3-molar guanidine-HCl, 20% Tween 20 solution, the cell lysate was mixed gently and incubated at 37 °C for 30 min. The genomic DNA was then extracted from this lysate using the Qiagen-tip 500 and protocol from the Qiagen Plasmid Maxi Kit (Qiagen, Valencia, CA). DNA concentration and purity were estimated by measuring OD<sub>260</sub> and OD<sub>280</sub>.

#### Cloning of *T. maritima* TM0298

The *T. maritima* TM0298 gene was amplified using *T. maritima* genomic DNA as the template, and oligonucleotides 5'-CGCATATGAAAGTACTTTTGATAG-3' (where CAT ATG creates an *Nde*I site) and 5'-CTCTCGAGAGAAA AAATTCCTTCATC-3' (where CTCTGAG creates a *Xho*I site) as the primers. The polymerase chain reaction (PCR) product was purified on an agarose gel and extracted using the Qiaex II Gel Extraction Kit (Qiagen) before being cloned into the pCR2.1-TOPO vector using the TOPO TA Cloning kit (Invitrogen). After sequence verification (at the Michigan State University Genomics Technology Support Facility), the TM0298 gene was subcloned into the *Nde*I and *Xho*I sites of pET24a(+) (Novagen) to yield plasmid pTmMtDH, from which TmMtDH is expressed with a C-terminal His<sub>6</sub>-tag. Plasmid DNA purification, restrictions, and cloning were performed using standard molecular biology protocols (Ausubel et al. 1993).

#### Protein expression and purification

To express TmMtDH, *E. coli* BL21(DE3) (pTmMtDH) was grown in 1 l SB kanamycin (50  $\mu$ g/ml) at 37 °C. TmMtDH expression was induced at an OD<sub>600</sub> of 1.4 by adding 0.6 mM isopropyl- $\beta$ -D-thiogalactoside (IPTG) and growing the culture for 16 more hours. After centrifugation (4,000 $\times$ g, 10 min), the cell pellet was resuspended (3 ml buffer per gram of wet pellet) in 50 mM 3-(*N*-morpholino) propanesulfonic acid (MOPS; pH 7.0) containing 5 mM  $\beta$ -mercaptoethanol plus EDTA-free complete mini protease inhibitor cocktail tablets (one tablet/10 ml buffer; Roche Diagnostics, Indianapolis, IN, USA). After adding 0.5 mg/ml (final concentration) lysozyme plus 500 U DNase I (Roche), the bacterial suspension was incubated at 37 °C for 1 h. Cells were disrupted by one pass through a French pressure cell using a pressure drop of 96 MPa. After centrifugation (25,000 $\times$ g, 30 min), the supernatant was heat-treated at 85 °C for 20 min, then centrifuged again (20,000 $\times$ g, 20 min).

The supernatant of the heat-treated extract was then loaded onto a 20-ml Ni-NTA agarose column (Qiagen). The column was washed with 20 volumes buffer A [20 mM Tris-HCl (pH 8.5), 100 mM KCl, 20 mM imidazole, 10 mM 2-mercaptoethanol, and 10% (v/v) glycerol], five volumes buffer B [20 mM Tris-HCl (pH 8.5), 1 M KCl, 10 mM 2-mercaptoethanol, and 10% (v/v) glycerol], and five volumes buffer C [20 mM Tris-HCl (pH 8.5), 100 mM KCl, 100 mM imidazole, 10 mM 2-mercaptoethanol, and 10% (v/v) glycerol]. The purified protein was dialyzed against 50 mM MOPS (pH 7.0) containing 5 mM  $\beta$ -mercaptoethanol and stored at -70 °C. Protein purity was assessed by sodium dodecyl sulfate polyacrylamide gel electrophoresis (SDS-PAGE) and staining with Coomassie Blue R-250. Protein concentration was quantified using the Bio-Rad (Hercules, CA, USA) protein assay dye reagent concentrate with bovine serum albumin as the standard.

*Lactobacillus reuteri* MtDH (LrMtDH) was expressed in *E. coli* BL21(DE3) (pLrMDH) and purified as described (Sasaki et al. 2005). The mutant derivative, 1F1, of *T. neapolitana* xylose isomerase was expressed in *E. coli* HB101(DE3) and purified as described (Sriprapundh et al. 2003). *T. neapolitana* xylose isomerase 1F1 is as stable as the wild-type enzyme and has  $V_{\max}$  and  $K_m$  values for glucose at 60 °C that are almost identical to those of the wild-type enzyme at 90 °C (Sriprapundh et al. 2003).

#### Determination of the molecular masses of *T. maritima* and *L. reuteri* MtDHs

The molecular masses of TmMtDH and LrMtDH were determined by gel filtration chromatography (flow rate, 0.5 ml/min) at 4 °C using an Akta FPLC chromatography system (GE Healthcare, Piscataway, NJ, USA) equipped with a Superdex 200 10/300 GL column [bed dimensions, 10 $\times$ 300 mm; void volume ( $V_o$ ), 8 ml] equilibrated with 50 mM sodium phosphate buffer containing 150 mM NaCl (pH 7.0). TmMtDH or LrMtDH (500  $\mu$ l at 4 mg/ml) was loaded on the column. Five hundred microliters each of 1 mg/ml carbonic anhydrase (29 kDa), 2.5 mg/ml bovine serum albumin (66 kDa), 1.5 mg/ml alcohol dehydrogenase (150 kDa), and 1 mg/ml  $\beta$ -amylase (200 kDa) were used as the protein standards (Sigma-Aldrich, St. Louis, MO, USA). The volume of the elution peak ( $V_e$ ) was determined, and the enzyme's molecular mass was estimated on a plot of log (molecular mass) versus  $V_e/V_o$ .

The molecular mass of TmMtDH was also determined by using analytical ultracentrifugation on a Protein Characterization System, ProteomeLab XL-I (Beckman Coulter, Fullerton, CA, USA). TmMtDH (83  $\mu$ M) in 50 mM MOPS (pH 7.0) containing 300 mM NaCl was centrifuged at 45,500 $\times$ g at 4 °C for 7 days. Scans were performed every

hour at 280 nm. The control cuvette contained only the buffer plus NaCl. Data were analyzed using in-house software.

### Enzyme assays

TmMtDH activity was routinely measured at 80 °C on a Cary 300 Bio UV/visible spectrophotometer (Varian Instruments, Walnut Creek, CA, USA) equipped with a Peltier system. The fructose reduction reaction (1 ml) contained 50 mM sodium phosphate buffer (pH 6.1), 200 mM fructose, 0.3 mM NADH, and 5.46 µg TmMtDH. The reaction was initiated by adding the enzyme to the reaction mixture that had been preheated to 80 °C for 5 min. The mannitol oxidation reaction (1 ml) contained 50 mM glycine buffer (pH 8.3), 0.5 mM NAD<sup>+</sup>, 200 mM mannitol, and 5.46 µg TmMtDH. Activity was recorded at 340 nm for 1 min. One unit of activity was defined as the amount of MtDH needed to consume (fructose reduction) or produce (mannitol oxidation) 1 µmol/min of NADH. Reduction reactions with substrates other than fructose (200 mM D-xylulose, D-xylulose, D-tagatose, L-sorbose, L-arabinose, L-threonine, acetaldehyde, or 2-butanone) were performed in the same conditions as for fructose. Oxidation reactions with substrates other than mannitol (with 200 mM sorbitol, xylitol, ethanol, or 2-butanol) were performed in the same conditions as for mannitol.

The effect of temperature on TmMtDH activity was also measured. For temperatures between 20 and 90 °C, activity was measured as described above. Above 80 °C, TmMtDH activity was measured using an end-point method. The reaction mixture minus the enzyme was preheated in an oil bath for 10 min. After adding the enzyme, the reaction mixture was further incubated for 15 s before stopping the reaction by transferring the tube to an ice-water bath for 10 min.

The effect of pH on TmMtDH activity was measured for both fructose reduction and mannitol oxidation at 80 °C. The fructose reduction (mannitol oxidation) reaction mixture contained 300 mM fructose (200 mM mannitol), 0.3 mM NADH (NAD<sup>+</sup>), and 5.46 µg/ml TmMtDH in 50 mM buffer. The buffers were sodium acetate (pH 4.5 to 5.5), sodium phosphate (pH 5.6 to 7.4), glycine (pH 7.5 to 8.5), and sodium carbonate (pH 9.0 to 10.2). All pH values were adjusted at room temperature. The  $\Delta pK_a/\Delta T$  values of glycine (1.375) and carbonate (0.5) were used to calculate pH values at 80 °C.

The kinetic parameters of TmMtDH at 80 °C were determined for fructose reduction (at pH 6.1) and mannitol oxidation (at pH 8.3). The  $K_m$  and  $V_{max}$  values for fructose (mannitol) were determined with 0.3 mM of NADH (NAD<sup>+</sup>). The  $K_m$  and  $V_{max}$  values for NAD(P)H and NAD(P)<sup>+</sup> were determined with 300 mM fructose and 200 mM mannitol, respectively.  $K_m$  and  $V_{max}$  values were

obtained through direct non-linear least squares curve fitting of the initial rate data to the Michaelis–Menten equation using Origin (Microcal Software, Northampton, MA, USA).

### Kinetic stability assays

To ensure inactivation data reproducibility, the enzyme (thawed on ice from –70 °C) was incubated for 5 min at 50 °C to restore its fully active conformation prior to inactivation experiments. TmMtDH kinetic thermostability was determined by incubating the enzyme [100 µl at 4.7 mg/ml in 0.1 M sodium phosphate (pH 7.5)] at 75, 80, 85, 90, and 95 °C for different periods of time in 100 µl screw-capped PCR tubes (catalog no. 72.733.050, Sarstedt, Newton, NC, USA). After heat inactivation, samples were immediately transferred to a room-temperature water bath for a few minutes. After centrifugation (16,000×g for 15 min), TmMtDH residual activity was determined with 60 µl of the supernatant using the 80 °C assay described above. The activity of the unheated protein was set as 100% residual activity. Non-linear curve fitting of the inactivation data was performed using the  $\chi^2$  minimization procedure of Origin. Half-lives ( $t_{1/2}$ ) were calculated using the equation  $t_{1/2} = \ln 2/k$ , where  $k$  is the inactivation constant.

### Analysis of TmMtDH's zinc content

The Zn<sup>2+</sup> content in TmMtDH was analyzed by inductively coupled plasma atomic emission spectroscopy (ICP-AES, MSU Diagnostic Center for Population and Animal Health) and by spectrophotometric titration. TmMtDH was extensively dialyzed against 40 mM HEPES/NaOH (pH 7.2) at 4 °C before both analyses. The dialysis buffer was used as the negative control. Three samples containing 70 µM TmMtDH were analyzed by ICP-AES, together with three dialysis buffer samples. This experiment was repeated twice with different enzyme preparations. TmMtDH (at 9.5 µM) was titrated spectrophotometrically with *p*-hydroxymercuriphenyl sulfonate (PMPS) in the presence of 4-(2-pyridilazo)resorcinol (PAR) in a Beckman DU650 spectrophotometer using a quartz microcuvette (1 cm path length) as described (Hunt et al. 1984). Zn<sup>2+</sup> was progressively released from TmMtDH by adding successive samples of 1 to 10 mM PMPS to 300 µl of TmMtDH in dialysis buffer containing 0.1 mM PAR. Absorbance at 250 and 500 nm was recorded 5 min after each PMPS addition. The cuvette containing the dialysis buffer plus TmMtDH and 0.1 mM PAR was used as the reference to zero the spectrophotometer.

To determine the effect of metals on TmMtDH activity, TmMtDH was incubated in 50 mM sodium phosphate buffer (pH 6.1) containing 10 mM EDTA for 20 min at 37 °C. Twenty millimolars of ZnCl<sub>2</sub>, CaCl<sub>2</sub>, CoCl<sub>2</sub>, MgCl<sub>2</sub>,

or  $MnCl_2$  were then added to the EDTA-treated enzyme, and the solution was incubated a further 20 min. Activity assays were performed at 80 °C before and after the addition of the metals using the standard assay described above.

### Two-step mannitol production from glucose

A 1-ml reaction mixture containing 100 mM phosphate buffer (pH 7.0), 180 mM glucose, 20 mM NADH, 0.5 mM  $CoCl_2$ , 5 mM  $MgSO_4$ , 0.772 mg *T. neapolitana* xylose isomerase 1F1, and 1 mg TmMtDH was incubated for 5 h at 60 °C ( $CoCl_2$  and  $MgSO_4$  were needed to optimize *T. neapolitana* xylose isomerase 1F1 activity). Fifty-microliter aliquots were removed from the reaction mixture at different times and immediately transferred into an ice bath to stop the reaction. The aliquots were boiled for 10 min to denature the enzymes, and they were centrifuged ( $16,000\times g$  for 10 min). The supernatants were transferred to high performance liquid chromatography (HPLC) vials (VWR, West Chester, PA, USA) for quantification by HPLC (Waters, Milford, MA, USA). Sugars and mannitol in 5- $\mu$ l samples were separated on a 300- $\times$ 7.8-mm Aminex HPX-87C carbohydrate analysis column (Bio-Rad) at 80°C with HPLC-grade water as the eluent at a flow rate of 0.6 ml/min. Peaks were detected with a Waters 410 refractive index detector. They were integrated using the Breeze HPLC software package (Waters). Standards were D-glucose,

D-fructose, D-mannose, and D-mannitol at concentrations ranging from 1 to 30 mM (mannitol) and 1 to 300 mM (glucose, fructose, and mannose).

### Results

#### Identification of a putative MtDH in *T. maritima*

Of all the protein sequences showing significant similarity to *L. mesenteroides* MtDH in a BLASTp search of the OMNIOME database, only one was from the proteome of a hyperthermophile, *T. maritima* TM0298. TM0298 is annotated as an alcohol dehydrogenase (ADH), but when it was used as the query sequence in a BLASTp search of GenBank, the best scores against proteins of known function were against the *L. mesenteroides* and *L. reuteri* MtDHs, with probabilities of  $9\times 10^{-38}$  and  $5\times 10^{-36}$ , respectively. TM0298 shares about 31% identity and 52% similarity with these two mesophilic MtDHs (Fig. 1). For this reason, we cloned *T. maritima* TM0298 and characterized its substrate specificity.

#### TM0298 expression and purification

*E. coli* BL21(DE3) (pTmMtDH) expressed high quantities of recombinant TM0298 after IPTG induction. Most of the

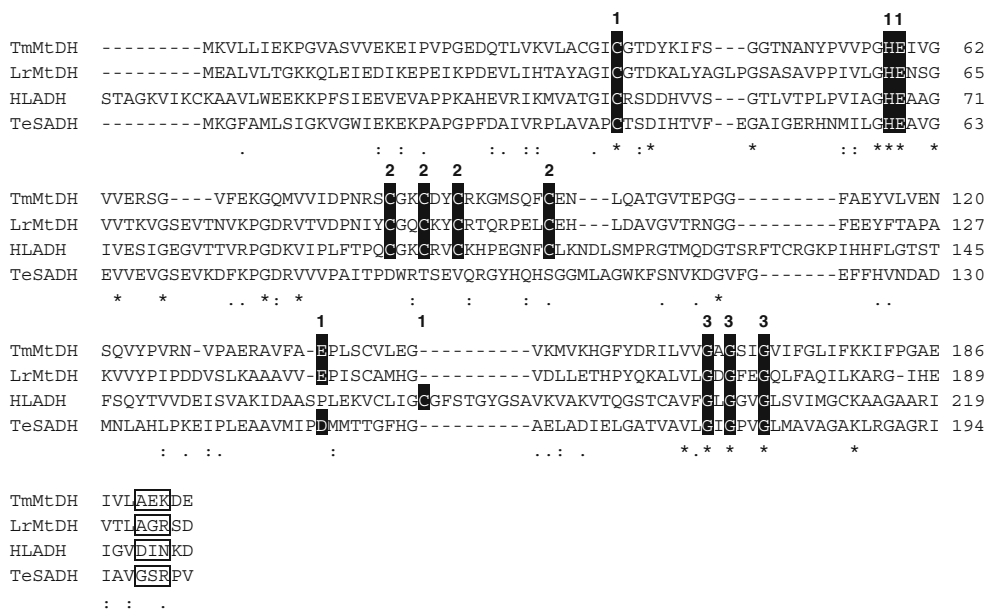


**Fig. 1** Partial alignment of TmMtDH with selected mannitol and alcohol dehydrogenases. TmMtDH, *T. maritima* MtDH (GenBank no. TM0298); LrMtDH, *Lactobacillus reuteri* MtDH (GenBank no. AAS55855); HLADH, horse liver ADH (GenBank no. P00327); and TeSADH, *Thermoanaerobacter ethanolicus* secondary ADH (GenBank no. EAO63648). Residues similar in all four enzymes are indicated by one or two dots; residues identical in the four enzymes

are indicated by a star. Residues highlighted in black are involved in catalytic  $Zn^{2+}$  binding (number 1 above the sequence alignment) or structural  $Zn^{2+}$  binding (number 2 above the sequence alignment), or they belong to the consensus cofactor binding region (number 3 above the sequence alignment). Boxed residues sequence involved in cofactor specificity

recombinant enzyme was present in the soluble fraction after centrifuging the crude extract. The 85 °C heat treatment was a highly efficient purification step. Additional purification on Ni-NTA agarose yielded a highly pure enzyme that migrated as a single, 34-kDa band on SDS-PAGE (data not shown). A purification buffer at pH 7.0 and protease inhibitors were essential for recovering the intact recombinant enzyme. TM0298 was sensitive to proteolytic degradation in purification protocols at pH 8.5 and in the absence of protease inhibitors (data not shown).

#### Characterization of TM0298 as an MtDH

The purified TM0298 was used in a series of enzyme assays to identify its substrate specificity. TM0298 had a specific activity of 54 U/mg protein at 80 °C with fructose as the substrate and NADH as the cofactor. It was also active on fructose with NADPH. TM0298 showed no detectable activity on glucose, xylose, threonine, arabinose, acetaldehyde, or 2-butanone (data not shown), but it showed 18% relative activity on D-xylulose, 29% on D-tagatose, and 5% on L-sorbose compared to 100% activity on D-fructose. In alcohol oxidation assays, TM0298 was active with mannitol as the substrate, but it showed no activity on sorbitol, xylitol, ethanol, or 2-butanol. Based on these results, TM0298 was subsequently called *T. maritima* MtDH (TmMtDH).

#### Effects of temperature and pH on TmMtDH activity and stability

TmMtDH optimally reduced fructose at pH values between 5.5 and 6.0, and it optimally oxidized mannitol between pH 8.3 and 8.6 (Fig. 2). The effect of temperature on TmMtDH activity was assayed by following the disappearance of NADH during the first 15 to 20 s of fructose reduction at temperatures ranging from 25 to 120 °C. In these assay conditions, TmMtDH was most active around 95 °C, above which activity decreased to 63% maximum activity at 120 °C (data not shown). The Arrhenius plot of TmMtDH activity was linear between 25 and 80 °C ( $R^2=0.997$ ; data not shown), with an activation energy of 64.6 kJ/mol. The thermostability of TmMtDH was tested at five temperatures. TmMtDH's kinetic inactivation followed a first-order reaction (Fig. 3), with inactivation constants of 0.0078 (75 °C), 0.0121 (80 °C), 0.0213 (85 °C), 0.0452 (90 °C), and 0.0992 (95 °C). Based on these inactivation constants, TmMtDH's calculated half-life was 91 min at 75 °C, 57 min at 80 °C, 32 min at 85 °C, 15 min at 90 °C, and 6 min at 95 °C. The Arrhenius plot of TmMtDH's kinetic inactivation (not shown) was linear, and a linear fit of the data ( $y=-16,917x+43.59$ ,  $R^2=0.988$ ) predicts an activation energy of 140.7 kJ/mol for TmMtDH inactivation. This high activation energy suggests

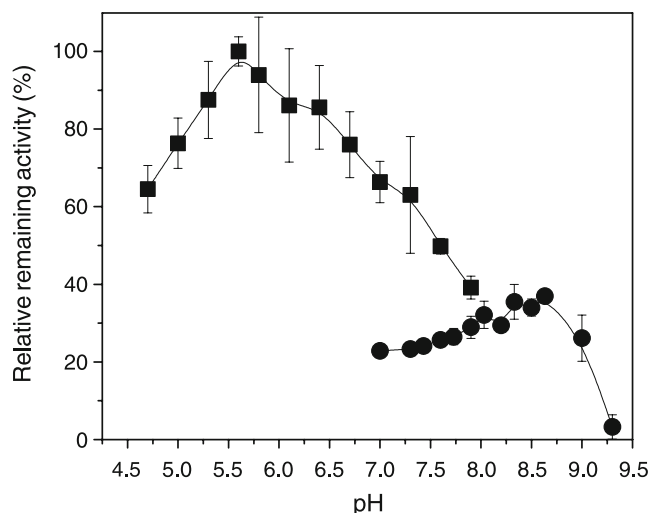


**Fig. 2** Effect of pH on TmMtDH activity at 80 °C. (■) fructose reduction and (●) mannitol oxidation

that TmMtDH is inactivated by unfolding rather than by a local mechanism (Tomazic and Klibanov 1988).

#### TmMtDH's kinetic parameters

TmMtDH's kinetic parameters were determined at 80 °C (Table 1). In fructose reduction, TmMtDH had a 3.6-fold lower  $K_m$  for NADH than for NADPH, and its catalytic efficiency with NADH was 2.2 times higher than with NADPH. In mannitol oxidation, TmMtDH's  $K_m$  value for  $\text{NAD}^+$  was 53 times lower than for  $\text{NADP}^+$ , and its catalytic efficiency with  $\text{NAD}^+$  was 33 times higher than with  $\text{NADP}^+$ . TmMtDH's  $K_m$  value for mannitol was one order of magnitude lower than for fructose. In preparation for bioelectrochemical reactor optimization studies (Hassler et al., manuscript in preparation), TmMtDH's kinetic parameters were also determined at 60 °C, pH 6.1 (Table 1). As expected,  $V_{\max}$  for fructose and NADH decreased 3.6- to 3.7-fold compared to 80 °C, but  $K_m$  values barely changed. In these conditions, the catalytic efficiency of mannitol oxidation was one tenth that of fructose reduction.

Mannitol behaved as a competitive inhibitor of fructose reduction. At 60 °C, TmMtDH's apparent  $K_m$  for fructose increased in the presence of increasing mannitol concentrations, whereas  $V_{\max}$  remained constant (Fig. 4). The inhibition constant for mannitol ( $K_i=99$  mM) was obtained by replotting the slopes of Fig. 4 versus mannitol concentration (not shown), yielding a straight line ( $y=0.02x+1.98$ ,  $R^2=0.9936$ ) whose intercept with the x axis was  $-K_i$ .

#### Zinc content and function in TmMtDH

TmMtDH belongs to the medium-chain dehydrogenase/reductase (MDR) family, whose members contain zero, one,

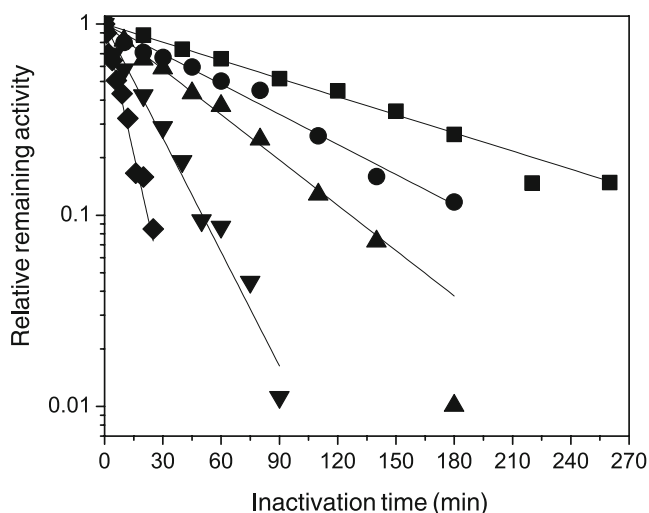


**Fig. 3** Effect of temperature on TmMtDH stability. (■) 75 °C, (●) 80 °C, (▲) 85 °C, (▼) 90 °C, and (◆) 95 °C

or two  $Zn^{2+}$  per subunit. Many MDRs contain a single, catalytic  $Zn^{2+}$  in their active site. Others, such as the horse liver ADH, contain a second  $Zn^{2+}$  at a structural site (Nordling et al. 2002). Because TmMtDH contains the conserved residues involved in catalytic and structural  $Zn^{2+}$  binding (Fig. 1), we measured TmMtDH's  $Zn^{2+}$  content. During spectroscopic titration of  $Zn^{2+}$ , PMPS was linearly incorporated into TmMtDH (followed at 250 nm), up to approximately 5 mol of PMPS per mole of enzyme. The  $\Delta A_{250}$  became constant at [PMPS]/[TmMtDH] ratios above 5. PMPS binding was accompanied by the release of  $Zn^{2+}$ , which immediately formed the complex  $(PAR)_2Zn^{2+}$  (detected at 500 nm). The  $(PAR)_2Zn^{2+}$  concentration increased linearly until the [PMPS]/[TmMtDH] ratio reached 5, after which it became constant, with a  $\Delta A_{500}$  of 0.43 (Fig. 5). With a molar absorption coefficient of  $6.6 \times 10^4 \text{ M}^{-1} \text{ min}^{-1}$  for  $(PAR)_2Zn^{2+}$  at 20 °C (Hunt et al. 1984), this  $\Delta A_{500}$  value corresponds to 0.69 mol of  $Zn^{2+}$ /subunit of enzyme. This result agrees with our ICP-AES result of 0.73 mol  $Zn^{2+}$  per mole TmMtDH. The ICP-AES results also indicated that

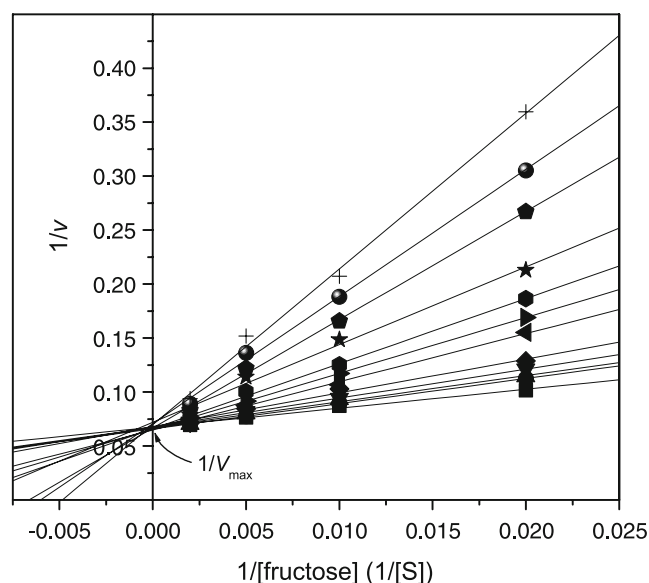


**Fig. 4** Inhibition of fructose reduction by mannitol: reciprocal plot of  $1/V$  versus  $1/[\text{fructose}]$  at different mannitol concentrations. Mannitol concentrations: (■) 0 mM, (●) 10 mM, (▲) 20 mM, (▼) 40 mM, (◆) 60 mM, (◄) 100 mM, (►) 150 mM, (⊙) 200 mM, (★) 300 mM, (⊕) 400 mM, (⊗) 500 mM, and (+) 600 mM

no other metal was present at a concentration close to stoichiometric amounts (data not shown), suggesting that Cys91, Cys94, Cys97, and Cys105 (Fig. 1) form either an empty or a non-functional structural metal binding site. These results indicate that TmMtDH contains a single  $Zn^{2+}$  cation.

To determine whether this  $Zn^{2+}$  is a catalytic metal, we tested the effects of EDTA and metals on activity. Activity of TmMtDH pretreated with 10 mM EDTA for 20 min at 37 °C decreased 96%. Adding 20 mM  $ZnCl_2$  to the EDTA-treated enzyme restored activity up to 80% of the control (enzyme not treated with EDTA). Adding 20 mM  $CoCl_2$  and 20 mM  $MnCl_2$  to the EDTA-treated enzyme restored activity up to 132% and 94% of the control, respectively. In contrast, adding 20 mM  $MgCl_2$  or  $CaCl_2$  did not increase the activity of the EDTA-treated enzyme. These results confirm that the single  $Zn^{2+}$  cation in TmMtDH is indeed a catalytic  $Zn^{2+}$ .

**Table 1** Kinetic parameters of *T. maritima* MtDH at 60 and 80 °C

Temperature (°C)	pH	Substrate	$V_{\max}$ (U/mg protein)	$K_m$ (mM)	Catalytic efficiency ( $V_{\max}/K_m$ )
80	6.1	D-Fructose <sup>a</sup>	58.70±0.86	50.97±2.58	1.15
80	6.1	NADH	58.24±1.23	0.048±0.003	1,213
80	6.1	NADPH	92.16±3.78	0.17±0.017	542
80	8.3	D-Mannitol <sup>a</sup>	37.85±0.77	5.51±0.74	6.87
80	8.3	NAD <sup>+</sup>	40.17±0.75	0.14±0.007	287
80	8.3	NADP <sup>+</sup>	64.57±1.12	7.5±0.53	8.61
60	6.1	D-Fructose <sup>a</sup>	15.88±0.29	50.00±3.4	0.32
60	6.1	NADH	15.98±0.45	0.037±0.004	432
60	6.1	D-Mannitol <sup>a</sup>	0.424±0.013	13.23±1.98	0.032

<sup>a</sup> Kinetic parameters for fructose and mannitol were determined with NADH and NAD<sup>+</sup>, respectively.

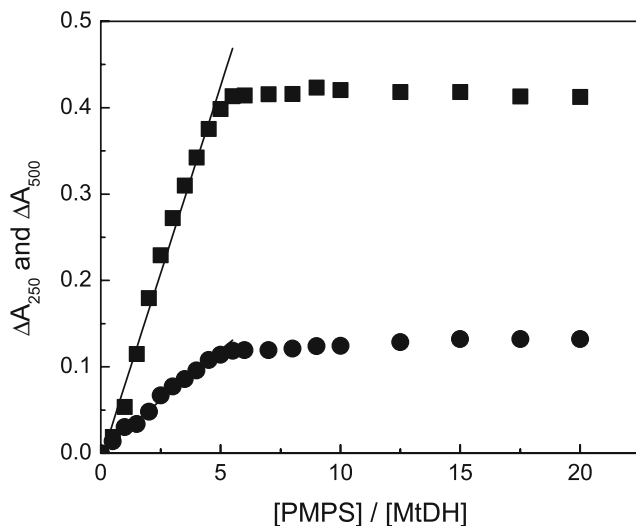


**Fig. 5** Titration of  $Zn^{2+}$  in TmMtDH with PMPS in the presence of PAR. (■)  $\Delta A_{500}$  and (●)  $\Delta A_{250}$

#### Determination of the oligomeric states of TmMtDH and LrMtDH

In gel filtration chromatography performed at 4 °C and at room temperature with different enzyme preparations and different enzyme concentrations, TmMtDH eluted as a single, sharp, symmetrical peak corresponding to a 120- to 143-kDa molecular mass (data not shown). With a subunit molecular weight of 34 kDa, these results suggest that TmMtDH is present in solution as a tetramer. These results were confirmed by analytical ultracentrifugation. TmMtDH sedimented with a sedimentation coefficient of 4.89 Svedbergs, corresponding to a protein mass of 120 kDa. The tetrameric form of TmMtDH was also likely the species that crystallized (Puttick et al. 2007).

Because TmMtDH and its mesophilic homologs from *L. mesenteroides* and *L. pseudomesenteroides* are tetrameric enzymes (Gründig et al. 1995; Woodyer et al. 2003), while *L. reuteri* MtDH was previously characterized as a dimer (Sasaki et al. 2005), gel filtration was repeated on LrMtDH at room temperature and at 4 °C in conditions identical to those used for TmMtDH. At room temperature, LrMtDH eluted predominantly as two peaks, corresponding to a dimer and a tetramer. It also showed minor peaks corresponding to an octamer (data not shown). When the eluted dimer or tetramer fraction was reloaded on the gel filtration column, it gave rise predominantly to a dimer or tetramer peak, respectively, suggesting that LrMtDH is present in the solution as a fixed mixture of dimer, tetramer, and octamer at room temperature (i.e., the dimer fraction does not repartition into dimer and tetramer, and likewise for the tetramer fraction). At 4 °C, LrMtDH eluted primarily as two peaks that were not well separated, with two minor peaks on either side. Because the overall elution

pattern was similar to the one from room temperature, the two main peaks probably correspond to the dimer and tetramer forms, even though each peak eluted approximately 1 ml earlier than at room temperature.

#### Two-step enzymatic transformation of glucose to mannitol with xylose isomerase and TmMtDH

Mannitol can be produced from glucose in two enzymatic steps. Xylose isomerase first produces fructose from glucose, and fructose is then reduced to mannitol by MtDH. To provide a first proof of concept that TmMtDH can be used together with xylose isomerase in a high-temperature process to convert glucose directly to mannitol, mannitol production from glucose was assayed in the presence of TmMtDH plus the *T. neapolitana* xylose isomerase mutant 1F1. As shown in Fig. 6, glucose concentration decreased with time from 200 to 84 mM, fructose concentration increased from 0 to 95 mM, and mannitol concentration increased from 0 to 19 mM. Because xylose isomerase has an epimerase activity that could produce mannose as a side product, mannose was included in the HPLC standards. At no time was mannose detected in the two-step enzymatic reaction. This observation agrees with the fact that the sum of the final glucose, fructose, and mannitol concentrations accounts for 99% of the initial glucose concentration.

#### Discussion

In this study, we cloned and characterized the thermostable, NAD-dependent TmMtDH. Most thermostable enzymes are

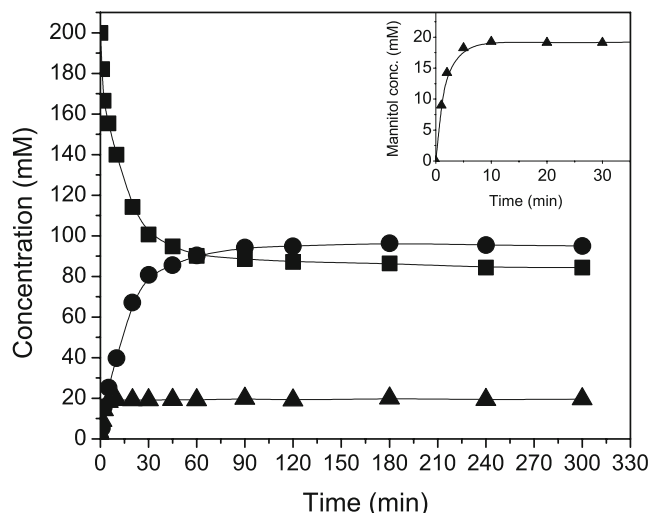


**Fig. 6** Mannitol production from glucose with TNXI 1F1 and TmMtDH at 60 °C. (■) glucose, (●) fructose, and (▲) mannitol



poorly active at low temperatures and only become highly active at higher temperatures where they become flexible enough for catalysis. They often have kinetic parameters at high temperatures that are of the same order of magnitude as those of mesophilic enzymes between 30 and 37 °C (Jaenicke 1991). TmMtDH is a typical hyperthermophilic enzyme: It shows no detectable activity at room temperature, and its activity at 40 °C is only 5% of its activity at 95 °C. In contrast, the mesophilic LrMtDH is 100% active at 37 °C, and it is completely inactivated by a 5-min heat treatment at 50 °C (Sasaki et al. 2005). TmMtDH's  $K_m$  and  $V_{max}$  on fructose at 80 °C are also close to those of mesophilic MtDHs between 25 and 37 °C (Aarnikunnas et al. 2002; Hahn et al. 2003; Korakli and Vogel 2003; Sasaki et al. 2005).

In the MDR family, it was suggested that the sequence G-x-G-x-x-G/A (Fig. 1) interacts with the diphosphate moiety of the NAD(P) cofactor (Carugo and Argos 1997). In NAD-specific enzymes, an acidic residue (D or E) is located approximately 18 residues downstream of this glycine motif. It is thought that this acidic residue is part of the nucleotide coenzyme binding site and that it provides a significant portion of cofactor specificity for NAD(H) (versus NADP(H)) by hydrogen bonding to one or both of the 2'- and 3'-hydroxyls of the adenine ribose. Basic residues in this region typically interact with the negatively charged 2'-phosphate of NADP(H)'s adenine ribose in NADP-dependent enzymes (Woodyer et al. 2003). TmMtDH contains the conserved sequence motif, G<sub>166</sub>-x-G<sub>168</sub>-x-x-G<sub>171</sub>, characteristic of NAD(P)-binding proteins (Fig. 1). Downstream of the glycine motif, the sequence Glu193-Lys194-Asp195-Glu196 might explain why TmMtDH is active with both NADH and NADPH, and why its catalytic efficiency for fructose reduction with NADH is 2.5 times higher than with NADPH. The side chain of Lys194 could form a salt bridge with the 2'-phosphate group of NADPH's ribose, but the negatively charged side chains of Glu193, Asp195, and Glu196 would repel this 2'-phosphate. In contrast, LrMtDH contains the sequence Gly196-Arg197-Ser198-Asp199 (Fig. 1). With a single negatively charged residue, LrMtDH has a six-time higher affinity for NADPH than for NADH (Sasaki et al. 2005), in contrast to TmMtDH, which has a 3.5-time higher affinity for NADH than for NADPH. This difference in cofactor specificity is also reflected in the two enzymes' catalytic efficiencies: LrMtDH's catalytic efficiency is 5.4 times higher with NADPH than with NADH (Sasaki et al. 2005), whereas TmMtDH's catalytic efficiency is 2.2 times higher with NADH than with NADPH. The higher affinity of TmMtDH for NADH than NADPH is another property of this enzyme that would be an advantage in the enzymatic production of mannitol, since NADH is significantly cheaper and more stable than NADPH (Wu et al. 1986).

The sequence alignment shown in Fig. 1 suggests that TmMtDH contains two zinc-binding sites per subunit: One catalytic Zn<sup>2+</sup> could bind to Cys37, His60, Glu61, and Glu152, and one structural Zn<sup>2+</sup> could bind to Cys91, Cys94, Cys97, and Cys105. These two sites have been shown to bind Zn<sup>2+</sup> in *Bemisia argentifolii* sorbitol dehydrogenase and horse liver ADH (Banfield et al. 2001; Vallee and Auld 1990). Our ICP-AES and Zn<sup>2+</sup> titration results suggest that TmMtDH contains only one Zn<sup>2+</sup> per subunit, though. Because TmMtDH activity is lost upon EDTA treatment and mostly restored by the subsequent addition of zinc, it is highly probable that the single Zn<sup>2+</sup> in TmMtDH is a catalytic zinc. Studies with the yeast ADH agree with this hypothesis: Removing the structural zinc in yeast ADH destabilized the enzyme without decreasing its catalytic activity (Magonet et al. 1992). LrMtDH also contains the four cysteines that bind a structural Zn<sup>2+</sup> in *B. argentifolii* sorbitol dehydrogenase and horse liver ADH. As was observed with TmMtDH, though, LrMtDH contains only a single catalytic Zn<sup>2+</sup> (Sasaki et al. 2005). Why TmMtDH and LrMtDH contain the structural Zn<sup>2+</sup> binding signature sequence without binding a structural Zn<sup>2+</sup> is a question open to speculation. Our consistent ICP-AES and PMPS titration results indicating a zinc content of no more than 0.7 Zn<sup>2+</sup> per TmMtDH subunit, instead of 1.0, are probably due to the fact that Zn<sup>2+</sup> cations were added neither during protein expression nor at any step of protein purification. Thus, all the protein-bound zinc must originate from impurities in the growth medium, glassware, and biological buffers (Vallee and Galdes 1984).

A variety of divalent metal ions, among them Co<sup>2+</sup>, Mn<sup>2+</sup>, Ni<sup>2+</sup>, Fe<sup>2+</sup>, Cu<sup>2+</sup>, and Cd<sup>2+</sup>, can restore the activity of EDTA-treated zinc metalloenzymes (Vallee and Galdes 1984). Zinc enzymes have, in fact, often been substituted with Co<sup>2+</sup> because of the electronic properties of Co<sup>2+</sup> and its use as a spectroscopic probe of metal coordination in proteins (Bertini and Luchinat 1984). Without a much more detailed study of metal binding in TmMtDH, which is not in the scope of this manuscript, it is not possible to explain why Co<sup>2+</sup> is better than Zn<sup>2+</sup> at restoring TmMtDH activity.

Of the four MDR, zinc-dependent MtDHs that have been cloned and characterized, LrMtDH is the only enzyme that exists in multiple oligomeric forms. The three other MtDHs are tetrameric. The *Lactobacillus sanfranciscensis* MtDH was determined to be a monomeric enzyme (Korakli and Vogel 2003), but because its gene has not been cloned and sequenced, it is still unclear whether *L. sanfranciscensis* MtDH belongs to the same enzyme family. It would be interesting to determine whether this enzyme is a monomeric member of the MDR family. It would also be interesting to study what unique structural features allow MDR dehydrogenases to be active in different oligomeric states.

The two-step enzymatic process shown in Fig. 6 provides the first proof of concept that xylose isomerase and MtDH can be combined in a single reaction vessel to produce mannitol directly from glucose. As expected in the absence of a cofactor-regenerating system, the final mannitol concentration only reached 19 mM. Indeed, fructose reduction to mannitol requires a stoichiometric amount of NADH, and only 20 mM NADH were included in the reaction. In these experimental conditions, mannitol production inevitably stopped once an equilibrium was reached between the concentrations of NADH, NAD<sup>+</sup>, fructose, and mannitol. Fructose accumulation in the reaction was expected as well because the reaction catalyzed by xylose isomerase is an equilibrium reaction that leads to a theoretical equilibrium at 60 °C of 50.7% fructose/49.3% glucose. This glucose-to-mannitol conversion process is being optimized in a bioelectrochemical reactor in which the two enzymes are co-immobilized on an electrode together with NADH and an electron mediator, and NADH is regenerated by an applied electrical potential. This work will be the subject of a separate paper (Hassler et al., manuscript in preparation).

**Acknowledgment** This work was supported by the National Research Initiative of the United States Department of Agriculture's Cooperative State Research, Education, and Extension Service, under grant number 2005-35504-16239. S. H. Song was supported in part by a grant from the Korea Research Foundation, Korean Government (MOEHRD; KRF-2006-214-D00050). L.T.J.D. is a Canada Research Chair in Structural Biochemistry. We thank Dr. J. G. Zeikus for his enthusiastic support and valuable discussions. We are grateful for the use of Dr. Jennifer Ekstrom's chromatography system. We thank Dr. Joe Leykam and Dr. William Wedemeyer for their assistance with analytical ultracentrifugation and analytical ultracentrifugation data analysis, respectively. We thank Dr. R. M. Kelly from North Carolina State University for sending us a preculture of *T. maritima*.

## References

- Aarnikunnas J, Ronnholm K, Palva A (2002) The mannitol dehydrogenase gene (*mdh*) from *Leuconostoc mesenteroides* is distinct from other known bacterial *mdh* genes. *Appl Microbiol Biotechnol* 59:665–671
- Albery W, Barlett P, Cass A, Sim K (1987) Amperometric enzyme electrodes. Part IV. An enzyme electrode for ethanol. *J Electroanal Chem* 218:127–134
- Ausubel FM, Brent R, Kingston RE, Moore DD, Seidman JG, Smith JA, Struhl K (eds) (1993) In: *Current protocols in molecular biology*. Greene Publishing, New York
- Banfield MJ, Salvucci ME, Baker EN, Smith CA (2001) Crystal structure of the NADP(H)-dependent ketose reductase from *Bemisia argentifolii* at 2.3 Å resolution. *J Mol Biol* 306:239–250
- Bardea A, Katz E, Buckmann AF, Willner I (1997) NAD-dependent enzyme electrodes electrical contact of cofactor dependent enzymes and electrodes. *J Am Chem Soc* 119:9114–9119
- Bertini I, Luchinat C (1984) High spin cobalt(II) as a probe for the investigation of metalloproteins. *Adv Inorg Biochem* 6:71–111
- Brünker P, Altenbuchner J, Kulbe KD, Mattes R (1997) Cloning, nucleotide sequence and expression of a mannitol dehydrogenase from *Pseudomonas fluorescens* DSM 50106 in *Escherichia coli*. *Biochim Biophys Acta* 1351:157–167
- Carugo O, Argos P (1997) NADP-dependent enzymes. I: conserved stereochemistry of cofactor binding. *Proteins* 28:10–28
- Chen T, Calabrese Barton S, Binyamin G, Gao Z, Zhang Y, Kim HH, Heller A (2001) A miniature biofuel cell. *J Am Chem Soc* 123:8630–8631
- Gründig B, Wittstock G, Rüdell U, Strehlitz B (1995) Mediator-modified electrodes for electrocatalytic oxidation of NADH. *J Electroanal Chem* 395:143–157
- Hahn G, Kaup B, Bringer-Meyer S, Sahn H (2003) A zinc-containing mannitol-2-dehydrogenase from *Leuconostoc pseudomesenteroides* ATCC 12291: purification of the enzyme and cloning of the gene. *Arch Microbiol* 179:101–107
- Hunt JB, Neece SH, Schachman HK, Ginsburg A (1984) Mercurial-promoted Zn<sup>2+</sup> release from *Escherichia coli* aspartate transcarbamoylase. *J Biol Chem* 259:14793–14803
- Jaegfeldt H, Torstensson A, Gorton I, Johansson G (1981) Catalytic oxidation of reduced nicotinamide adenine dinucleotide by graphite electrodes modified with adsorbed aromatic containing catechol functionalities. *Anal Chem* 53:1979–1982
- Jaenicke R (1991) Protein stability and molecular adaptation to extreme conditions. *Eur J Biochem* 202:715–728
- Johnson MR, Montero CI, Chou CJ, Shockley KR, Kelly RM (2006) The *Thermotoga maritima* phenotype is impacted by syntrophic interaction with *Methanococcus jannaschii* in hyperthermophilic coculture. *Appl Environ Microbiol* 72:811–818
- Jörnvall H, von Bahr-Lindstrom H, Jeffery J (1984) Extensive variations and basic features in the alcohol dehydrogenase-sorbitol dehydrogenase family. *Eur J Biochem* 140:17–23
- Jörnvall H, Persson B, Jeffery J (1987) Characteristics of alcohol/polyol dehydrogenases. The zinc-containing long-chain alcohol dehydrogenases. *Eur J Biochem* 167:195–201
- Karyakin AA, Bobrova OA, Karyakina EE (1995) Electroreduction of NAD<sup>+</sup> to enzymatically active NADH at poly(neutral red) modified electrodes. *J Electroanal Chem* 399:179–184
- Kaup B, Bringer-Meyer S, Sahn H (2005) D-Mannitol formation from D-glucose in a whole-cell biotransformation with recombinant *Escherichia coli*. *Appl Microbiol Biotechnol* 69:397–403
- Korakli M, Vogel RF (2003) Purification and characterization of mannitol dehydrogenase from *Lactobacillus sanfranciscensis*. *FEMS Microbiol Lett* 220:281–286
- Kulbe KD, Schwab U, Gudernatsch W (1987) Enzyme-catalyzed production of mannitol and gluconic acid. Product recovery by various procedures. *Ann N Y Acad Sci* 506:552–568
- Laurinavicius V, Kurtinaitiene B, Gureviciene V, Boguslavsky L, Geng L, Skotheim T (1996) Amperometric glyceride biosensor. *Anal Chem Acta* 330:159–166
- Le AS, Mulderrig KB (2001) Sorbitol and mannitol. In: O'Brien Nabors L (ed) *Alternative sweeteners*. Marcel Dekker, New York
- Magonet E, Hayen P, Delforge D, Delaive E, Remacle J (1992) Importance of the structural zinc atom for the stability of yeast alcohol dehydrogenase. *Biochem J* 287:361–365
- Munteanu FD, Kubota LT, Gorton L (2001) Effect of pH on the catalytic electrooxidation of NADH using different two-electron mediators immobilised on zirconium phosphate. *J Electroanal Chem* 509:2–10
- Nordling E, Jörnvall H, Persson B (2002) Medium-chain dehydrogenases/reductases (MDR). *Eur J Biochem* 269:4267–4276
- Ohtani M, Kuwabata S, Yoneyama H (1997) Electrochemical oxidation of reduced nicotinamide coenzymes at Au electrodes modified with phenothiazine derivative monolayers. *J Electroanal Chem* 422:45–54

- Pariante F, Lorenzo E, Tobalina F, Abruna HD (1995) Aldehyde biosensor based on the determination of NADH enzymatically generated by aldehyde dehydrogenase. *Anal Chem* 67:3936–3944
- Park DH, Zeikus JG (2003) Improved fuel cell and electrode designs for producing electricity from microbial degradation. *Biotechnol Bioeng* 8:348–355
- Park DH, Laivenieks M, Guettler MV, Jain MK, Zeikus JG (1999) Microbial utilization of electrically reduced neutral red as the sole electron donor for growth and metabolite production. *Appl Environ Microbiol* 65:2912–2917
- Park DH, Vieille C, Zeikus JG (2003) Bioelectrocatalysts: engineered oxidoreductase system for utilization of fumarate reductase in chemical synthesis, detection, and fuel cells. *Appl Biochem Biotechnol* 111:41–53
- Prodomidis MI, Karayannis MI (2002) Enzyme based amperometric biosensors for food analysis. *Electroanalysis* 14:241–261
- Puttick P, Vieille C, Song SH, Fodje MN, Grochulski P, Delbaere LTJ (2007) Crystallization, preliminary X-ray diffraction and structure analysis of *Thermotoga maritima* mannitol dehydrogenase. *Acta Crystallogr F* 63:350–352
- Sasaki Y, Laivenieks M, Zeikus JG (2005) *Lactobacillus reuteri* ATCC 53608 *mdh* gene cloning and recombinant mannitol dehydrogenase characterization. *Appl Microbiol Biotechnol* 68:36–41
- Schafer A, Stein MA, Schneider KH, Giffhorn F (1997) Mannitol dehydrogenase from *Rhodobacter sphaeroides* Si4: subcloning, overexpression in *Escherichia coli* and characterization of the recombinant enzyme. *Appl Microbiol Biotechnol* 48:47–52
- Schneider KH, Giffhorn F (1989) Purification and properties of a polyol dehydrogenase from the phototrophic bacterium *Rhodobacter sphaeroides*. *Eur J Biochem* 184:15–19
- Schneider KH, Giffhorn F, Kaplan S (1993) Cloning, nucleotide sequence and characterization of the mannitol dehydrogenase gene from *Rhodobacter sphaeroides*. *J Gen Microbiol* 139:2475–2484
- Slatner M, Nidetzky B, Kulbe KD (1999) Kinetic study of the catalytic mechanism of mannitol dehydrogenase from *Pseudomonas fluorescens*. *Biochemistry* 38:10489–10498
- Soetaert W, Buchholz K, Vandamme EJ (1995) Production of D-mannitol and D-lactic acid by fermentation with *Leuconostoc mesenteroides*. *Agro Food Ind Hi Tech* 6:41–44
- Soetaert W, Vanhooren P, Vandamme E (1999) Production of mannitol by fermentation methods. *Biotechnology* 10:261–275
- Sriprapundh D, Vieille C, Zeikus JG (2003) Directed evolution of *Thermotoga neapolitana* xylose isomerase: high activity on glucose at low temperature and low pH. *Protein Eng* 16:683–690
- Stoop JM, Mooibroek H (1998) Cloning and characterization of NADP-mannitol dehydrogenase cDNA from the button mushroom, *Agaricus bisporus*, and its expression in response to NaCl stress. *Appl Environ Microbiol* 64:4689–4696
- Tomazic SJ, Klibanov AM (1988) Mechanisms of irreversible thermal inactivation of *Bacillus*  $\alpha$ -amylases. *J Biol Chem* 263:3086–3091
- Vallee BL, Auld DS (1990) Zinc coordination, function, structure of zinc enzymes and other proteins. *Biochemistry* 29:5648–5659
- Vallee BL, Galdes A (1984) The metallochemistry of zinc enzymes. *Adv Enzymol Relat Areas Mol Biol* 56:283–430
- van der Donk WA, Zhao H (2003) Recent developments in pyridine nucleotide regeneration. *Curr Opin Biotechnol* 14:421–426
- von Weymar N, Kiviharju K, Leisola M (2002) High-level production of D-mannitol with membrane cell-recycle bioreactor. *J Ind Microbiol Biotechnol* 29:44–49
- Willner I, Katz E (2000) Integration of layered redox proteins and conductive supports for bioelectronic applications. *Angew Chem Int Ed* 39:1180–1218
- Woodyer R, van der Donk WA, Zhao H (2003) Relaxing the nicotinamide cofactor specificity of phosphite dehydrogenase by rational design. *Biochemistry* 42:11604–11614
- Wu JT, Wu LH, Knight JA (1986) Stability of NADPH: effect of various factors on the kinetics of degradation. *Clin Chem* 32:314–319